OPEN ACCESS

Saudi Journal of Civil Engineering

Abbreviated Key Title: Saudi J Civ Eng
ISSN 2523-2657 (Print) |ISSN 2523-2231 (Online)
Scholars Middle East Publishers, Dubai, United Arab Emirates
Journal homepage: https://saudijournals.com/journal/sjce/home

Original Research Article

Synergistic Corrosion Inhibition of Mild Steel in Acidic Media Using Eichhornia Crassipes Extract and Zinc Oxide Nanoparticles: Electrochemical and Surface Morphology Insights

Oke O. O[1,2]*, Oloruntoba D.T.[2], Olaseinde O.A.[2]

[1]Mineral and Petroleum Resources Engineering Department, The Federal Polytechnic Ado Ekiti, Nigeria
[2]Department of Metallurgical and Materials Engineering, Federal University of Technology, Akure

DOI: https://doi.org/10.36348/sjce.2026.v10i11.002 | **Received:** 12.07.2026 | **Accepted:** 05.09.2026 | **Published:** 07.11.2026

***Corresponding author:** Oke O. O
Mineral and Petroleum Resources Engineering Department, The Federal Polytechnic Ado Ekiti, Nigeria

Abstract

This work offers a detailed examination of the corrosion inhibiting action of an aqueous extract derived from *Eichhornia crassipes* (water hyacinth), employed in conjunction with zinc oxide (ZnO) nanoparticles, as a hybrid green formulation for mild steel exposed to 1.0 M HCl. The study confronts two interrelated objectives: reducing metallic deterioration in highly acidic media and repurposing an invasive aquatic weed into a usable material resource. A series of electrochemical measurements, including impedance spectroscopy and potentiodynamic polarization, were carried out over a range of extract to nanoparticle ratios. The optimal composition 0.5 g of plant extract combined with 0.1 g of ZnO yielded a maximum efficiency of 55.73%, a value substantially higher than that recorded for either constituent alone, thus confirming a cooperative enhancement effect. Polarization data further revealed that the combined system acts as a mixed inhibitor, moderating both anodic metal dissolution and cathodic hydrogen discharge. Microscopic and spectroscopic surface analyses (SEM–EDX) provided clear evidence of a dense and well adhered film covering the steel substrate, which curtailed both localized pitting and widespread surface loss. The presence of naturally occurring phytochemicals tentatively identified as flavonoids, tannins, and phenolics together with the inherent surface activity of ZnO nanoparticles, appears to facilitate improved adsorption and prolonged film resilience. This chemical interplay forms the basis for the observed rise in protective performance. Beyond the laboratory findings, the study underscores the practical viability of transforming an ecological nuisance into an inexpensive, non-hazardous inhibitor, positioning it as a plausible substitute for conventional but hazardous compounds such as chromates and synthetic organic inhibitors. In a broader context, the results support the principles of waste valorization and resource cycling, while pointing toward future work on nanoparticle surface modification and improved extraction protocols.

Keywords: Water hyacinth, ZnO nanoparticles, Mild steel, Electrochemical impedance spectroscopy, green inhibitors.

Copyright © 2026 The Author(s): This is an open-access article distributed under the terms of the Creative Commons Attribution **4.0 International License (CC BY-NC 4.0)** which permits unrestricted use, distribution, and reproduction in any medium for non-commercial use provided the original author and source are credited.

INTRODUCTION

Corrosion constitutes a persistent and costly challenge across numerous industrial sectors and infrastructural systems, giving rise to substantial economic losses and concomitant environmental harm. This electrochemical phenomenon has long been recognized as a principal threat to the longevity and reliability of engineering structures, particularly affecting metallic components including vehicle body panels, transmission pipelines, and rotating machinery that are routinely exposed to atmospheric moisture and oxidizing agents. Given that the chemical interaction between metals and their surrounding environment cannot be entirely prevented, the management of corrosion remains an enduring operational concern (Zhang & Li, 2026).

Mild steel, owing to its favourable combination of low production cost, excellent machinability, high toughness, and appreciable ductility, finds extensive application in the construction, automotive, and manufacturing industries. Nevertheless, this same material exhibits pronounced susceptibility to acidic attack, which compromises its mechanical integrity and frequently precipitates premature component failure. Conventional remedial approaches including electrodeposited coatings, surface passivation

treatments, and mechanical deformation techniques such as extrusion and cold rolling have been employed to alleviate this vulnerability, though each carries inherent limitations in terms of cost, scalability, or long-term effectiveness (Adeyemi *et al*., 2026).

Within aggressive acidic environments, the corrosion of mild steel has persistently challenged sectors such as petroleum refining, chemical processing, and civil infrastructure. Traditional organic and inorganic inhibitors, while demonstrably effective, are increasingly scrutinized for their elevated toxicity, high procurement costs, and detrimental ecological footprints. This has generated a pressing demand for sustainable, environmentally benign alternatives capable of affording dependable protection under corrosive service conditions (Zhang & Li, 2026).

In response, naturally derived substances particularly plant-based extracts have attracted considerable research interest as prospective green corrosion inhibitors. Among these, *Eichhornia crassipes* (commonly known as water hyacinth) has emerged as a notable candidate, owing to its prolific abundance in tropical freshwater systems and its documented phytochemical complexity. Prior investigations have attributed the inhibitory activity of such extracts to the presence of polar organic molecules, including alkaloids, flavonoids, tannins, and various phenolic compounds, which are known to adsorb onto metal surfaces and impede charge-transfer processes (Chen *et al.,* 2025). Despite these encouraging preliminary observations, the precise efficiency thresholds and underlying mechanistic pathways governing water hyacinth-mediated corrosion suppression remain insufficiently characterized.

The broader shift toward environmentally sustainable corrosion mitigation has intensified scrutiny of plant derived inhibitors as viable substitutes for toxic conventional agents, such as chromates and phosphates. These bio-based alternatives offer distinct advantages, including biodegradability, low mammalian toxicity, and a rich repertoire of heteroatom bearing functional groups that facilitate surface chemisorption (Chen *et al.,* 2025). Within this context, water hyacinth an invasive macrophyte that has colonized numerous Nigerian watercourses since the mid-1980s presents a compelling case for valorization. Its aggressive proliferation has historically obstructed navigational channels and curtailed artisanal fishing activities, yet this same abundance renders it a readily accessible and low-cost feedstock for inhibitor formulation (Chen *et al*., 2025). Recent experimental work has further demonstrated that hybrid composites combining water hyacinth extracts with zinc oxide (ZnO) nanoparticles exhibit enhanced corrosion resistance for steel in acidic chloride media, attributed to the anodic inhibition characteristics of ZnO, which complement the adsorption-driven protection afforded by the organic phytochemicals (Okafor & Suleiman, 2026).

Accordingly, the present study investigates the synergistic corrosion inhibition performance of water hyacinth leaf extract, in combination with ZnO, as a green inhibitor system for mild steel immersed in acidic solution. Through the systematic application of electrochemical impedance spectroscopy and potentiodynamic polarization measurements, this work aims to contribute empirical insights to the expanding literature on sustainable corrosion protection strategies, while also bridging the gap between laboratory-scale findings and practical industrial applicability.

MATERIALS AND METHODS

Raw Materials

The materials used for this study include water hyacinth plant (WHP), ZnO powder, and Mild Steel. The metallic samples were procured as scraps at the engineering complex, Federal Polytechnic Ado and the chemical composition of each of the material was determined at the laboratory of Arts et Métiers Institute of Technology, Metz, France. Zinc Oxide was purchased from a chemical dealer in the Ado metropolis. The corrodant (1.0 M HCl) needed was also purchased at the same place. The WHP was obtained from riverine areas at Ilaje Okitipupa, Ondo State, Nigeria.

Methodology

Preparation of Water Hyacinth (Eichhornia crassipes) Extracts

Fresh samples of the aquatic macrophyte water hyacinth (*Eichhornia crassipes*) were harvested from the riverine regions of Ilaje in Ondo State, Nigeria. The collected leaves were thoroughly cleaned and subjected to oven-drying at 60°C to remove moisture (Singh *et al*., 2020). To maximize the extraction of active phytochemical ingredients such as alkaloids, flavonoids, and tannins the dried leaves were pulverized into very fine particles using a mechanical grinding machine, which provides a large surface area for the solvent interaction.

Following the extraction protocol established by Singh *et al*. (2020), a portion of the pulverized plant was soaked in ethanol for 48 hours. The resulting aqueous mixture was then filtered and decanted, and the excess ethanol was allowed to evaporate at room temperature to yield a concentrated nano-powder extract. This extract was subsequently used to prepare inhibitory solutions at varying concentrations of 0.1–0.5 g/L in 1.0 M HCl environment to evaluate its effectiveness in mitigating the corrosion of metallic substrates like mild steel.

Preparation of Mild Steel Specimens

Mild steel rods with the composition shown in Table 1 were machined into coupons (3mm × 10 mm diameter). Each coupon was polished with emery paper to achieve a smooth surface, cleaned with distilled water, and soldered with copper wire for electrical connection. The steel rod sample shown in table 1 primarily

composed of iron (95.99%), along with carbon (0.25%), silicon (0.75%), manganese (2.3%), phosphorus (0.06%), copper (0.27%), and chromium (0.31%). This composition is typical for mild steel, particularly due to the carbon percentage. The analysis indicates that this is a low alloy carbon steel, featuring modest levels of manganese, silicon, and copper. When exposed to hydrochloric acid (HCl), the high iron content and low chromium/molybdenum ratio make it particularly vulnerable to uniform corrosion from aggressive chloride and hydrogen ions, with manganese and silicon providing minimal protection. Overall, this steel demonstrates poor resistance to acids, highlighting the need for protective coatings or inhibitors to enhance its durability.

Table 1: Elemental Composition of Mild Steel

Element	C	P	Mn	Cr	Mo	Si	S	Cu	Fe
Composition	0.25	0.06	2.3	0.31	0.02	0.75	0.05	0.27	95.99

Preparation of Water Hyacinth (*Eichhornia crassipes*) Inhibitor Extract (WHE)

Fresh water hyacinth (*Eichhornia crassipes*) was harvested from Ilaje Riverine areas of Ondo State, Nigeria. The water hyacinth plant plucked were placed inside an oven for drying at a temp of 60^0 C for 5 hours. The dried plant was pulverized to very fine particles using a mechanical grinding machine (RM 200 Mortal Grinder). The pulverized plant gave room for large surface area to extract higher concentration of active ingredients responsible for corrosion inhibition. The pulverized *Eichhornia crassipes* plant was measured into a beaker containing 500 ml of ethanol and was left for 48 hours. The aqueous solution in the beaker was filtered, decanted and excess ethanol was allowed to evaporate following the method of Singh *et al.,* 2020. The powder of the extract was used in this research.

ZnO -Water Hyacinth Extract (WHE) Mix Ratio

ZnO powder was procured from a laboratory in Ado metropolis. Different concentrations (0.1–0.5 g) were prepared in beakers combined with water hyacinth extract in varying ratios:

- Run 1: 0.1 g ZnO + 0.5 g extract
- Run 2: 0.2 g ZnO + 0.4 g extract
- Run 3: 0.3 g ZnO + 0.3 g extract
- Run 4: 0.4 g ZnO + 0.2 g extract
- Run 5: 0.5 g ZnO + 0.1 g extract
- Run 6: Blank (no inhibitor)

2.2.5 Determination of the Phytochemical Constituents

Biochemical tests were done to check the presence and the quantity of different phytochemicals such as flavonoids, steroids, tannin, alkaloids, anthraquinone, cardiac glycosides, phytobalatin and terpenoid in the ethanol extracted leave of water hyacinth and this was carried out by simple qualitative and quantitative methods as shown in Tables 2 and 3.

Table 2: Phytochemical Screening of Water Hyacinth (Qualitative screening)

Secondary Metabolite	Inference
Alkaloid	$_{++}$ve
Phenol	$_{+++}$ve
Flavonoid	$_{+++}$ve
Tannin	$_{+}$ve
Terpernoid	$_{+}$ve

Table 3: Phytochemical screening of water hyacinth (Quantitative screening)

Secondary metabolite	Constituent
Alkaloid	1.9
Tannin	1.4
Flavonoid	3.9
Terpernoid	3.25
Phenon	5.0

Gas Chromatography-Mass Spectrometry (GC-MS)

Gas chromatography-mass spectrometry (GC-MS) analysis of the water hyacinth plant extract (WHPE) was carried out in a combined gas chromatograph system and mass spectrophotometer, fitted with a HP-5 MS fused silica column (5%) phenyl methyl siloxane 30.0m ×250 µm, film thickness 0.25 µm), interfaced with 5675C Inert MSD with Triple-Axis detector. Helium gas was used as carrier gas and adjusted to column velocity flow of 1.0 ml/min. The chromatogram of water Hyacinth extract is shown in figure 1. While the identified components is shown in table 4.

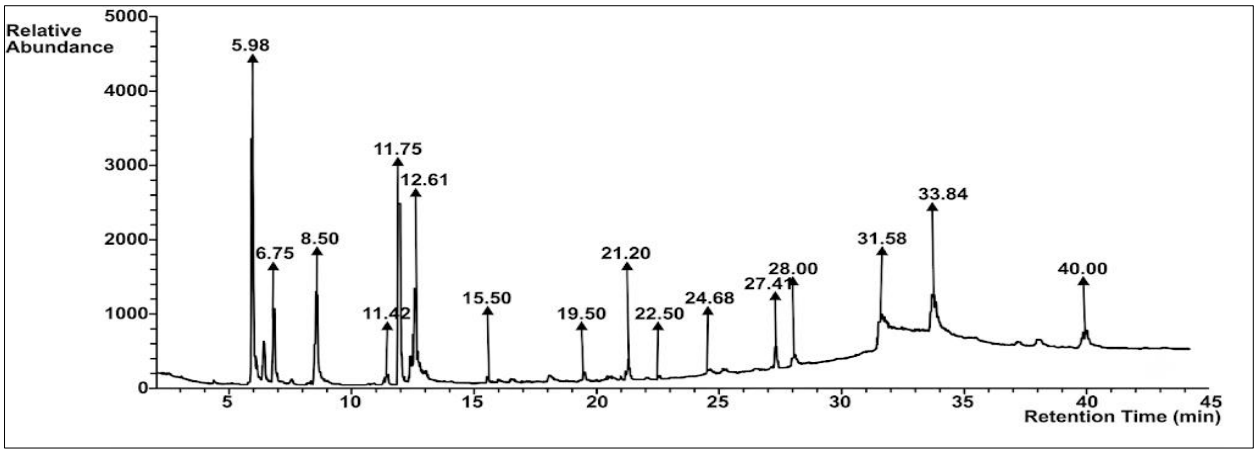


Figure 1: GCMS Chromatogram of Water Hyacinth Extract

Table 4: Identified Component In Water Hyacinth Extract (Whe)

Peak #	RT	Compound Detected	Mol. Formula	MW	Peak Area %	Comp %wt	m/z	Structures
1	1.76	2-Propanone	C_3H_6O	58	25.76	8.42	41, 43, 58	
2	3.48	2-Propanone	$C_3H_6O_4$	166	9.85	9.57	41, 43, 58	
3	6.33	1,2-Benzenedicarboxylic acid	$C_8H_6O_4$	166	9.85	9.57	43, 78, 166	
4	9.25	2-Benzenic acid	$C_{12}H_{12}O_4$	166	8.30	9.55	43, 78, 166	
5	10.18	β-Fitane	$C_{18}H_{12}O_3$	156	7.35	2.97	43, 87, 166	
6	10.53	1-Bitane-dienoic acid	$C_{18}H_{32}O_2$	280	1.14	2.03	43, 87, 280	
7	13.29	(10E,12Z)-octadeca-10,12-dienoic acid	$C_{18}H_{32}O_2$	280	1.14	2.03	43, 87, 280	
8	15.85	1-Butoxy-1-isobutoxy-butane	$C_{18}H_{32}O_2$	280	1.14	2.03	43, 87, 280	
9	16.63	3-vinylobutane	$C_{18}H_{32}O_2$	280	0.99	2.03	43, 87, 320	
10	19.30	2-Blyl-butane	$C_{28}H_{50}O_2$	374	1.00	1.68	43, 87, 320	
11	22.16	β-kyanene	$C_{29}H_{50}O_2$	414	1.04	2.03	43, 87, 370	
12	13.35	λ-Sitostene	$C_{29}H_{50}O_2$	400	0.69	2.66	43, 87, 440	
14	14.00	1-Stamohylbutane	$C_{29}H_{50}O_2$	473	1.67	3.62	43, 87, 433	
15	15.10	4-Tnextipod-pohybranic acid	$C_{29}H_{40}O_2$	414		-	477	
16	16.00	β-Sitosterol	$C_{29}H_{50}O$	414	6.21	5.56	43, 107, 414	

2.2.7 Functional Group Determination (WHP)

FT-IR **(Fourier transform infrared)** spectra was carried out to analyze the structure of the surface film and the functional group. The infrared reflectance spectra of AA5052 after immersing in solution with additives. The displayed infrared absorption peaks were summarized in Table 5 and Figure 2.

Table 5: Fourier Transform Infrared Spectroscopy (FTIR)Results

Run #	Peak Wavelength (cm^{-1})	Transmittance (%)	Assignment	Functional group
1	3183.07	19.86	O-H Stretching vibration which is absorbed on the sample	Hydroxyl group
2	1642.99	18.03	C=O stretching vibration of proteins (Amide I)	Amide I
3	1496.04	20.15	-C-O-C, Stretching vibrational mode of the α-1,4 glucosidic linkage	Carboxylic
4	1182.03	36.98	C–O stretching vibrations	Aldehydes
5	1062.87	36.56	CH_2 and CH_3 stretching vibrations from proteins	Amide I
6	815.20	29.13	CH bending vibrations	Alkanes
7	750.01	30.18	C-Cl, C-Br, C-I stretching vibrations	Alkyl halides

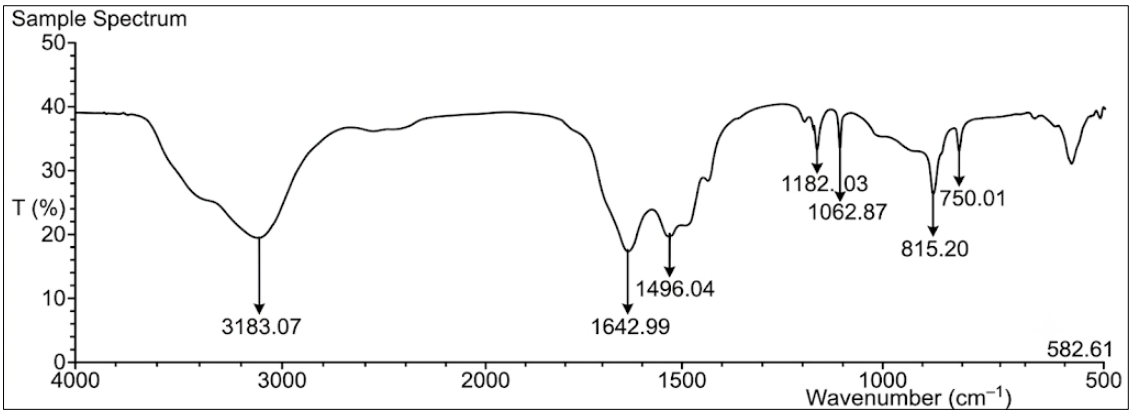


Figure 2: FTIR analysis of Water Hyacinth Extract

Electrochemical Studies

Electrochemical measurements were conducted using a three-electrode cell system with mild steel as the working electrode, a graphite rod as the counter electrode, and a saturated calomel electrode (SCE) as the reference. The cell was cleaned after each run with chromic-sulphuric acid, rinsed with distilled water, and conditioned with the test solution.

Electrochemical impedance spectroscopy (EIS) was performed in the frequency range 0.01 Hz ≤ f ≤ 3 × 10 Hz with a 10mV amplitude signal. Potentiodynamic polarization curves were recorded at a scan rate of 20 mV/min. The inhibition efficiency (%IE) was calculated in the equation 1:

$$IE\% = \frac{Io - I}{Io} \times 100 \qquad (1)$$

where Io and I are the corrosion current densities without and with inhibitor, respectively (Adeyemi *et al*, 2026).

Surface Morphology Analysis

After exposure to test solutions, mild steel samples were dried and examined using SEM and EDX. SEM provided insights into surface morphology, while EDX determined the elemental composition of the protective layer formed on the steel surface (Chen *et al*., 2025).

RESULTS AND DISCUSSION

Results

Characterization Process

Figure 1 and Table 4 present the GC-MS chromatograph analysis of WHE and the identified compounds of WHE with their retention time, peak percentage area, compound name, compound weight and structures. The identified compounds contain oxygen as a heteroatom in their structures. This property confirms the inhibitive potentials of the plant extract of *water hyacinth* as corrosion inhibitor. The identified compounds are 2-Propanone, (25.76%); furfural (8.33), 1,2- Benzene dicarboxylic acid (9.85%); Tetradecanoic acid (1.51 %); n- Hexadecanoic acid (11.36%), Octadecanoic acid (9.46), octadeca-10,12-dienoic acid (1.14%), 1-Butoxy-1-isobutoxy-butane (1.29%), 9,12-Octadecadienoic acid (Z, Z)-(2.12%). GC–MS results strongly influence how we understand and control corrosion because the chemical compounds identified in the chromatogram often act either as corrosion inhibitors**.** For example, polar organic molecules such as phenols, amines, or fatty acids detected by GC–MS can adsorb onto metal surfaces and form protective films, thereby reducing acid attack and slowing down corrosion (Schwarzbauer *et al., 2020)*. Ofuyekpone *et al*. (2025) demonstrated that bio-based extracts identified by GC–MS contained both polar and non-polar compounds that enhanced corrosion inhibition in chloride environments (Izionworu *et al*.,2020)

Figure 2 revealed the FTIR spectrum of WHE while Table 5 shows the absorption band located at 3183.07 cm^{-1} is linked to the stretching vibrations of hydroxyl groups. The absorption band at 1642.99 cm^{-1} is associated with the stretching vibration of protein bonds. The adsorption band at 1496.04 cm^{-1} is responsible for the stretching vibration mode of the α-1,4 glucosidic linkage in -C-O-C of the carboxylic group. The absorption band at 1182.03 cm^{-1} arises from the stretching vibrations of C–O in aldehydes. The absorption bands at 1062.87 cm^{-1} are related to the CH_2 and CH_3 stretching vibrations from proteins in Amide I. The absorption band at 815.20 cm^{-1} corresponds to the stretching vibration of CH bending vibrations. The absorption band at 750.01 cm^{-1} can be attributed to the stretching vibrations of C-Cl, C-Br, and C-I' The FTIR spectrum displays distinct absorption peaks that correspond to O–H, C=O, and C=C stretching vibrations. The broad peak at 3183.07 cm^{-1} confirms the presence of hydroxyl groups, while the peak at 1642.99 cm^{-1} is linked to amide and carbonyl functionalities. Peaks near 1182.03 cm^{-1} and 1062.87 cm^{-1} are associated with C–O stretching, indicating the presence of alcohols and ethers. These functional groups are known to participate in chemisorption through electron donation from lone pairs of oxygen and nitrogen atoms to the vacant d-orbitals of iron. The presence of halogenated compounds at 750.01 cm^{-1} further supports the ability of the extract to form stable complexes that block active corrosion sites. The FTIR data thus corroborate the GC–MS findings,

confirming that bioactive compounds within water hyacinth extract contribute to the inhibition mechanism via surface adsorption and complex film formation. The presence of the -OH group or catechol can support the binding of organic molecules onto the surface of the materials (Davilal *et al.,2022).*

Table 2 and 3 present the qualitative and quantitative phytochemical analysis of water hyacinth which identified the presence of alkaloids, phenols, flavonoids, tannins, and terpenoids, all of which are compounds well-known for their potential to inhibit corrosion. Alkaloids and flavonoids function as adsorption inhibitors by donating lone pairs of electrons from nitrogen and oxygen atoms to the metal surface, thus forming protective complexes. Phenols and tannins provide antioxidant and chelating properties that stabilize passive films and mitigate oxidative degradation, while terpenoids promote the formation of hydrophobic films, thereby limiting localized corrosion. The lack of saponins and quinones indicates that the inhibition mechanism primarily depends on adsorption and antioxidation rather than foaming or redox activity. Recent research supports these conclusions. Akinfaloye *et al*. 2024, demonstrated that water hyacinth extract decreased corrosion in crude oil carbon steel tanks due to the synergistic effects of alkaloids and polyphenols creating protective layers.

Table 6: Potentiodynamic Polarization result

S/n	Concentration	E corr (v)	j-corr (a/cm2)	Corrosion rate (mm/yr)	polarizatio resistance (ω)	ba (v/dec)	Bc (v/dec)	%IE
1	Blank	-0.60735	0.0040284	46.81	4.3923	0.078628	0.084555	0.0
2	0.1g Plant/0.5g ZnO	-0.59852	0.0036757	42.711	5.4092	0.091356	0.091769	8.76
3	0.2g Plant/0.4g ZnO	-0.61226	0.0027456	31.904	6.5827	0.082908	0.083556	31.78
4	0.3g Plant/0.3g ZnO	-0.60507	0.002462	28.608	7.2282	0.084295	0.079734	38.88
5	0.4g Plant/0.2g ZnO	-0.59947	0.0023566	27.384	7.6924	0.086852	0.080361	41.49
6	0.5g Plant/0.1g ZnO	-0.59488	0.0021178	24.609	7.383	0.078282	0.066662	47.42

The potentiodynamic polarization data in Table 6 highlight the corrosion inhibition behavior of *Eichhornia crassipes* (water hyacinth) extract combined with zinc oxide (ZnO) for mild steel in 1.0 M HCl solution. The blank sample exhibited the highest corrosion current density (jcorr=0.0040284 A/cm2) and corrosion rate (46.81 mm/yr), confirming the aggressive nature of the acidic medium. The low polarization resistance (4.39 Ω) further indicates poor corrosion resistance in the absence of inhibitors which is as a result of mild steel lacking significant alloying elements like chromium or nickel that provide corrosion resistance (Conniff & Tewolde 2026).

With the addition of inhibitor systems, a clear reduction in corrosion current density and corrosion rate was observed. At the optimum concentration (0.5 g plant extract/0.1 g ZnO), the corrosion current density decreased to 0.0021178 A/cm², while the corrosion rate dropped to 24.61 mm/yr. This condition corresponded to the highest inhibition efficiency (47.42%) and an increase in polarization resistance (7.38 Ω). These results suggest that the adsorption of phytochemicals from water hyacinth onto the steel surface forms a protective barrier and Inhibitors create a hydrophobic layer that prevents chloride ions from reaching the steel surface., reducing chloride ion penetration (Al-Moubaraki & Al-Harthi, 2025).

The relatively small shifts in corrosion potential (Ecorr) across all concentrations indicate that the inhibitor acts as a mixed-type inhibitor, affecting both anodic and cathodic reactions. The stability of anodic (ba) and cathodic (bc) Tafel slopes supports the hypothesis that inhibition occurs primarily through surface adsorption rather than altering the fundamental electrochemical pathways (Singh *et al*,.2025).

The increase in polarization resistance with higher inhibitor concentrations demonstrates the synergistic effect of ZnO and water hyacinth extract. ZnO contributes to anodic inhibition, while phytochemicals such as flavonoids and phenolic compounds provide cathodic protection by blocking active sites on the steel surface (Chidiebere *et al.,* 2026).

Overall, the findings confirm that water hyacinth extract, particularly in combination with ZnO, can serve as an effective green corrosion inhibitor for mild steel in acidic environments. The maximum inhibition efficiency of 47.42% underscores its potential as a sustainable alternative to conventional toxic inhibitors, aligning with the growing emphasis on eco-friendly corrosion protection strategies (Kumar *et al.,* 2026).

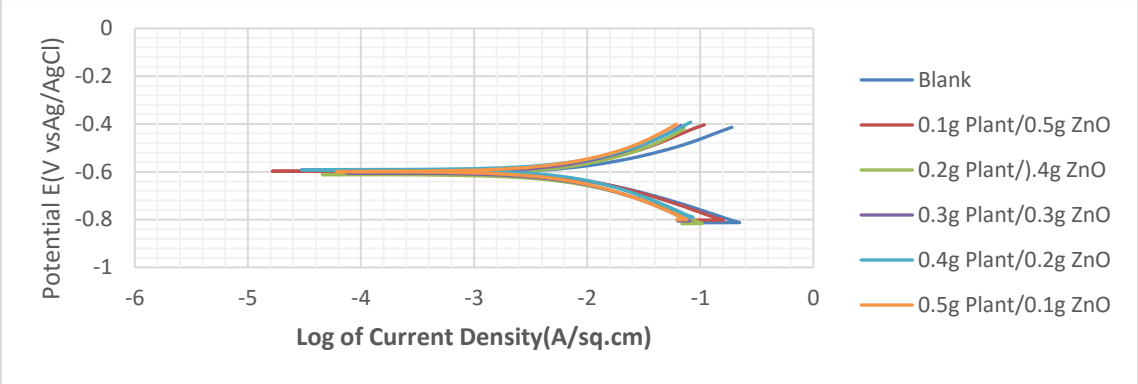


Figure 3: Potentiodynamic Polarisation chart showing behavior of immersed steel in varying concentration of inhibitor in the 1.0M Hcl

Table 7: Electrochemical impedance spectroscopy (EIS) result

Concentration	Rs (ohm)	Rct (ohm)	Yo1(S*s^a)	n1	Rf (ohm)	Yo2(S*s^a)	n2	%IE
Blank	6.36E-01	9.0	8.78E-04	8.88E-01	8.66E-01	5.83E-04	8.69E-01	0
0.1gPlant/0.5g ZnO	1.60E-01	10.03	9.71E-04	9.38E-01	9.464	2.53E-03	6.67E-01	10.26
0.2gPlant/0.4g ZnO	3.70E-01	16.89	8.52E-04	8.97E-01	1.88	4.93E-04	9.03E-01	46.71
0.3gPlant/0.3g ZnO	2.18E-01	13.51	1.15E-03	9.01E-01	5.878	5.50E-04	7.72E-01	33.38
0.4g Plant/0.2g ZnO	6.35E-01	19.51	3.86E-04	9.60E-01	8.62E01	1.07E-03	8.04E-01	53.86
0.5g Plant/0.1g ZnO	3.03E-01	20.33	7.40E-04	9.48E-01	3.221	2.86E-03	1	55.73

Discussion of Electrochemical Impedance Spectroscopy (EIS) Results

The electrochemical impedance spectroscopy (EIS) data presented in Table 7 provide further evidence of the corrosion inhibition efficiency of *Eichhornia crassipes* (water hyacinth) extract in combination with zinc oxide (ZnO) for mild steel in 1.0 M HCl solution.

For the blank sample, the charge transfer resistance (Rct) was lowest (9.0 Ω), indicating rapid electron transfer and severe corrosion. The double-layer capacitance values (Yo1 and Yo2) were relatively high, reflecting poor surface coverage and active corrosion sites.

With the addition of inhibitors, a significant increase in Rct was observed, accompanied by a reduction in capacitance values. At the optimum concentration (0.5 g plant extract/0.1 g ZnO), Rct increased to 20.33 Ω, while the inhibition efficiency reached 55.73%. This improvement suggests that the inhibitor molecules adsorbed onto the steel surface, reducing the active area available for corrosion reactions and enhancing the protective film's stability (Obot *et al*,. 2025).

The values of the constant phase element (n1 and n2) remained close to unity across most concentrations, indicating that the electrode/electrolyte interface behaved nearly like an ideal capacitor. This behavior is consistent with the formation of a uniform protective layer on the steel surface, which reduces charge transfer and stabilizes the electrochemical system (El-Haddad *et al,.*2025).

Interestingly, the synergistic effect of ZnO and water hyacinth extract is evident in the progressive increase in film resistance (Rf) with higher extract concentrations. ZnO likely contributes to anodic inhibition, while phytochemicals such as flavonoids and phenolic compounds enhance cathodic protection by blocking active sites. This dual mechanism aligns with recent findings on hybrid organic-inorganic inhibitors that combine adsorption with passivation effects (Singh *et al.,* 2020).

Overall, the EIS results corroborate the potentiodynamic polarization findings, confirming that water hyacinth extract, particularly in combination with ZnO, acts as a mixed-type inhibitor. The maximum inhibition efficiency of 55.73% demonstrates its potential as a sustainable and eco-friendly alternative to conventional inhibitors in acidic environments (Al-Sabagh *et al*,.2026)

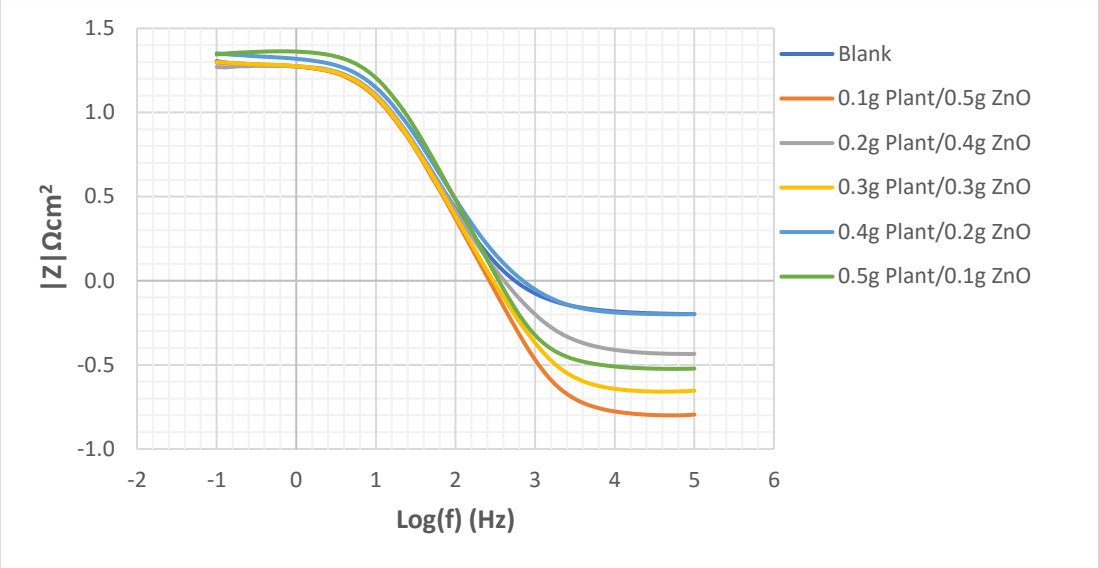


Figure 4: Bode plot of MS 1.0M Hcl in the varying concentrations of Water hyacinth extracts and Zinc oxide

The figure 4 revealed that in 1 M HCl solution, mild steel is highly susceptible to corrosion as a result of hydrogen evolution and the action of chloride ions. The Bode impedance plot shows the effect of plant extract/ZnO composites on the corrosion behaviour of the steel. The blank sample exhibits relatively high impedance, indicating limited surface protection and continued corrosion. With increasing ZnO content, the impedance decreases, suggesting increased charge transfer and lower resistance to corrosion. In contrast, increasing the proportion of plant extract results in higher impedance, which can be attributed to the formation of an organic film on the steel surface. This film acts as a barrier to charge transfer and consequently reduces the corrosion rate. The 0.3 g plant extract/0.3 g ZnO mixture gives an intermediate impedance response, indicating a combined effect of both materials, with ZnO contributing to the surface interaction while the plant extract helps to protect and stabilize the steel surface (Saeidlou, 2026).

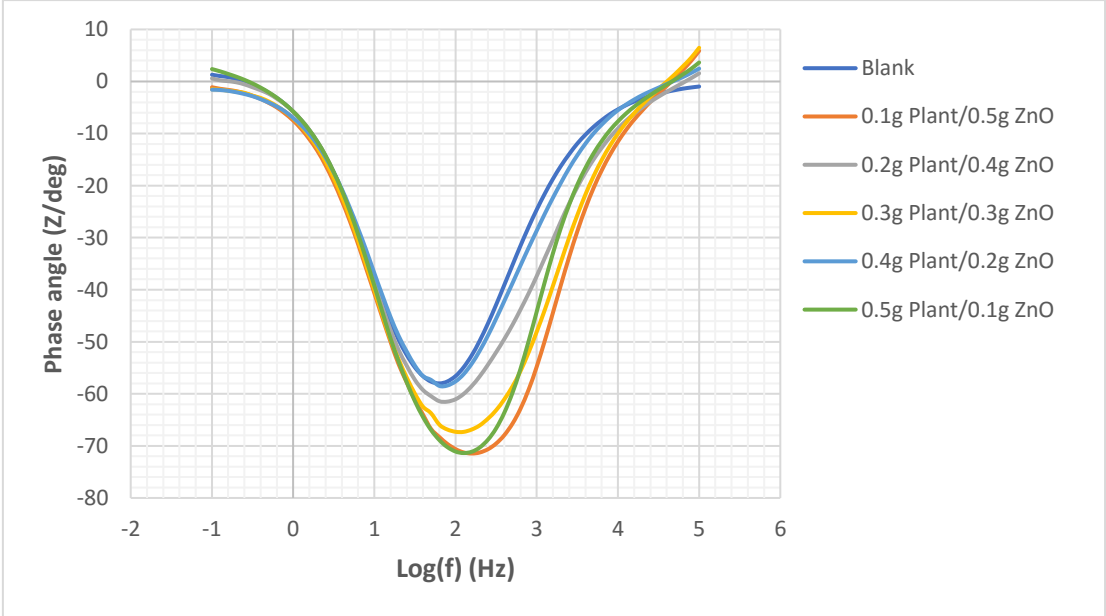


Figure 5: Phase angle Bode spectra of MS in 1.0M Hcl in the varying concentrations of Water hyacinth extracts and Zinc oxide

Figure 5 Presents Bode phase angle plot highlights how plant/ZnO composites modify this behavior. ZnO-rich mixtures show lower phase angles, reflecting faster charge transfer and weaker inhibition. Plant-rich mixtures display more negative phase angles, consistent with organic film adsorption that blocks charge transfer and slows corrosion. The 0.3g Plant/0.3g ZnO mixture demonstrates intermediate performance, suggesting a synergistic effect: ZnO interacts with the

steel surface while the plant extract stabilizes and shields it, thereby reducing the overall corrosion rate.

Figure 6 Presents the Nyquist plot illustrates how plant/ZnO composites affect this process. The blank sample shows a large semicircle, indicating high charge transfer resistance and active corrosion. ZnO-rich mixtures reduce semicircle diameter, reflecting faster electron transfer and weaker inhibition. Plant-rich mixtures enlarge the semicircle, consistent with protective organic film adsorption that hinders charge transfer and slows corrosion. The 0.3g Plant/0.3g ZnO mixture demonstrates intermediate behavior, suggesting synergistic protection where ZnO interacts with the steel surface while the plant extract stabilizes and shields it (Ramesh, & Rajendran 2024).

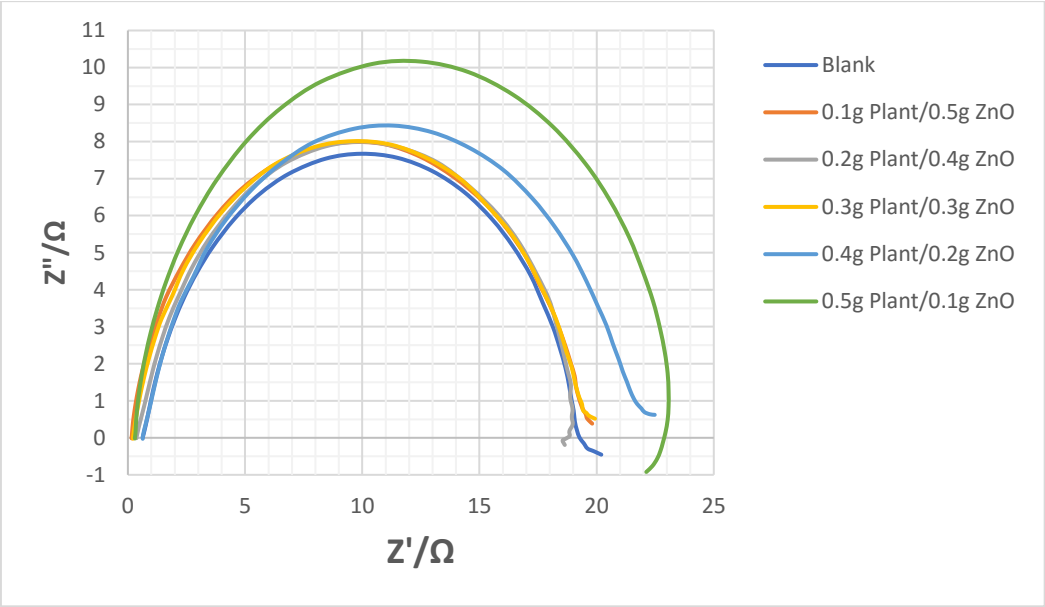


Figure 6: Nyquist plot of MS in 1.0M HCl in the varying concentration of the water hyacinth extracts. EIS results show the development of a protective layer of inhibitor molecule over the metal surface

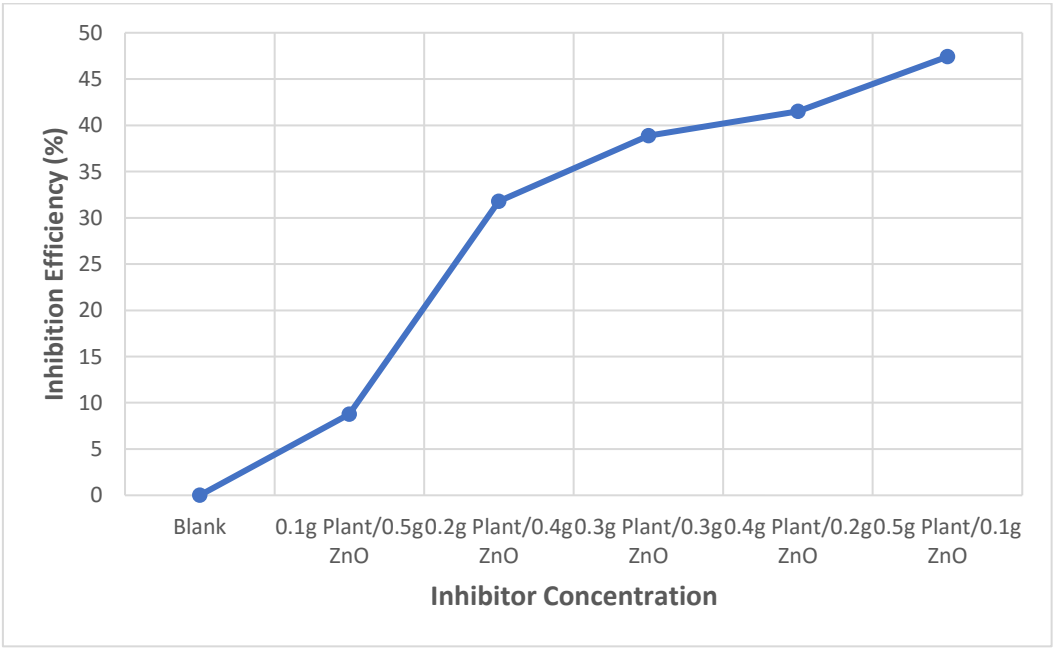


Figure 7: Potentiodynamic Polarization Result Plot of Inhibition Efficiency against inhibitor concentration of MS in 1.0M Hcl in the varying concentrations of Water hyacinth extracts and Zinc oxide

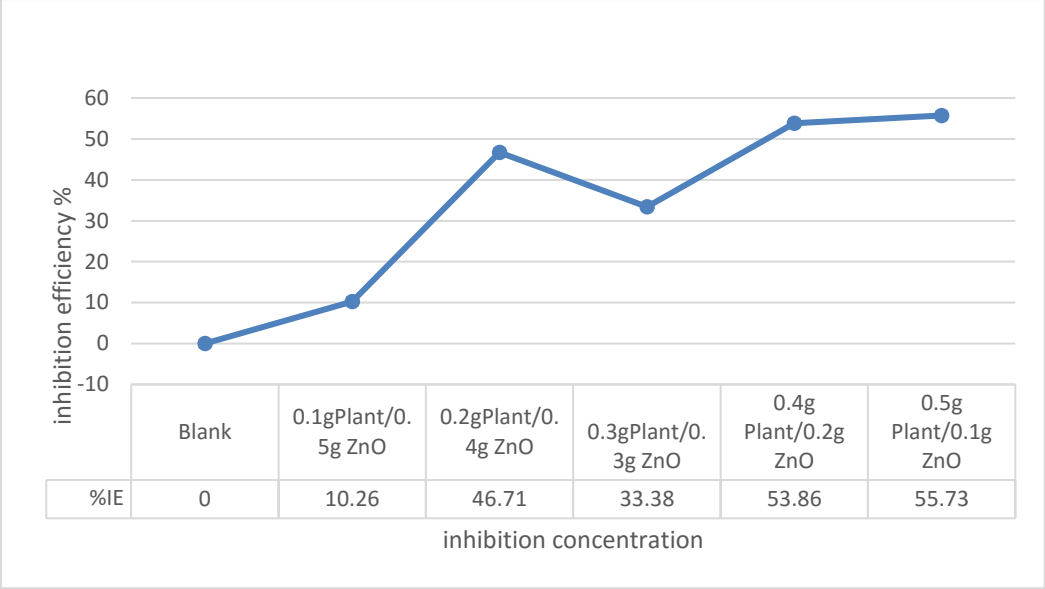
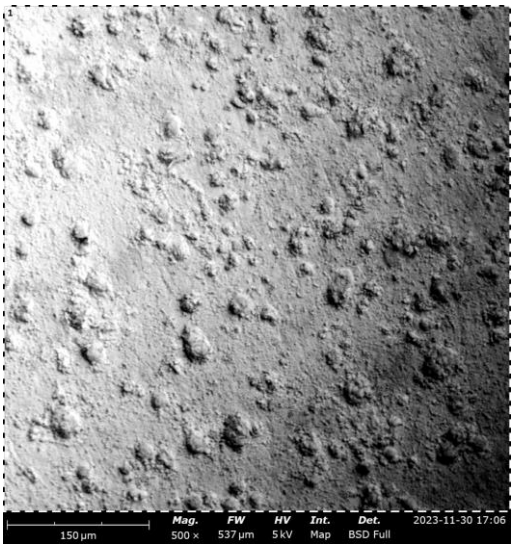


Figure 8: Electrochemical impedance spectroscopy (EIS) Result Plot of Inhibition Efficiency against inhibitor concentration of MS in 1.0M Hcl in the varying concentrations of Water hyacinth extracts and Zinc oxide



Element Number	Element Symbol	Element Name	Atomic Conc.	Weight Conc.
8	O	Oxygen	45.48	18.77
26	Fe	Iron	39.22	56.50
22	Ti	Titanium	11.10	13.71
52	Te	Tellurium	3.26	10.74
6	C	Carbon	0.94	0.29

Figure 9: SEM Micrograph of the blank Sample (FOV: 537 µm, Mode: 5kV - Map, Detector: BSD Full, Time: NOV 30 2023 17:06) and with its chemical composition

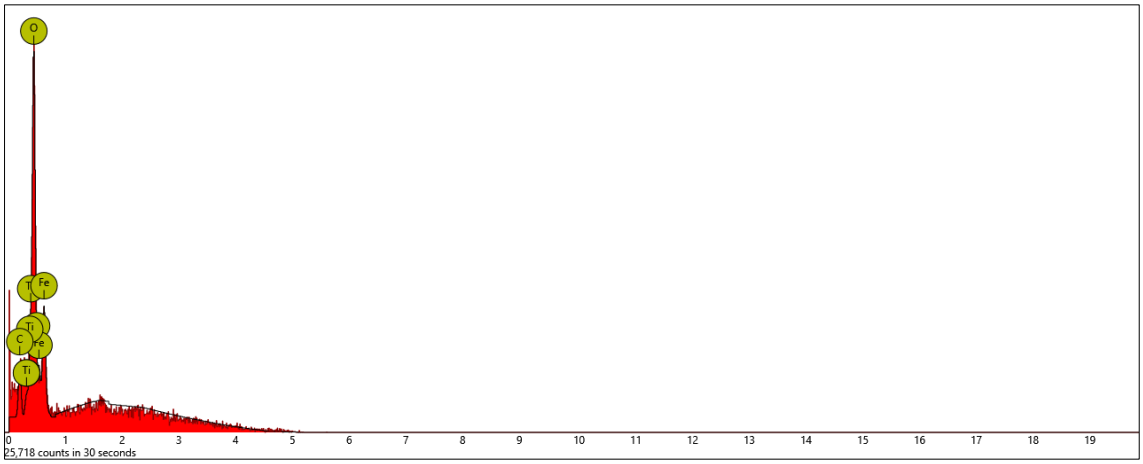
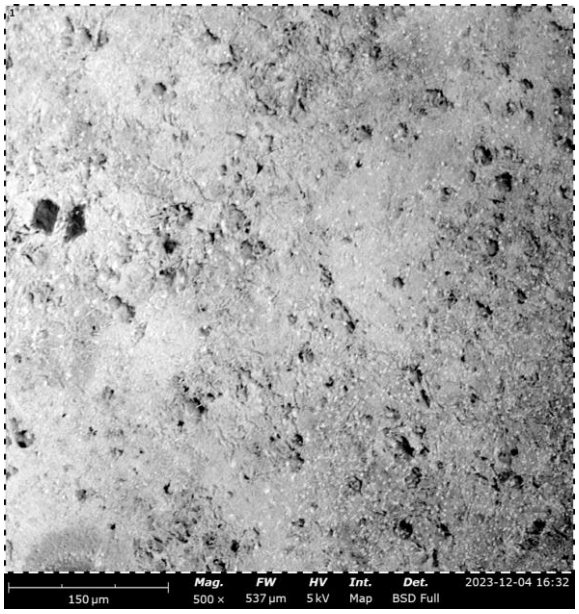


Figure 10: EDX Spectrum of the blank Sample



Element Number	Element Symbol	Element Name	Atomic Conc.	Weight Conc.
8	O	Oxygen	30.21	7.00
26	Fe	Iron	25.61	20.70
22	Ti	Titanium	21.39	14.83
82	Pb	Lead	15.84	47.51
59	Pr	Praseodymium	4.69	9.57
6	C	Carbon	2.27	0.39

Figure 11: SEM Micrograph of the highest immersed concentrated Sample (FOV: 537 µm, Mode: 5kV - Map, Detector: BSD Full, Time: DEC 4 2023 16:32) and with its chemical composition

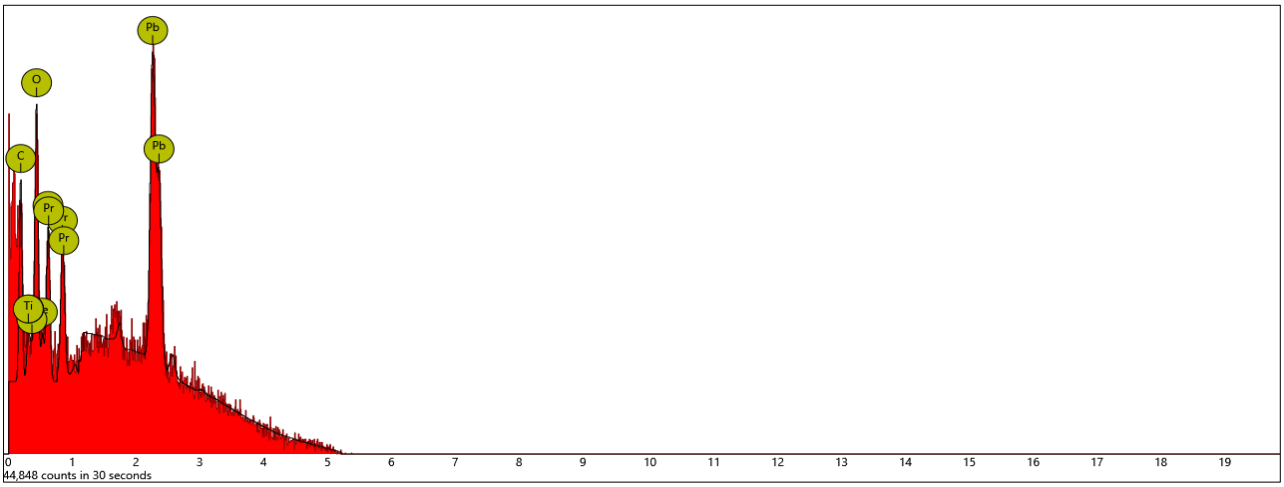


Figure 12: EDX Spectrum of the highest immersed concentrated Sample

Surface Morphology Analysis

The morphology of the mild steel surface was examined using scanning electron microscopy (SEM) after immersion in 1.0 M HCl solution, both in the absence and presence of the highest concentration of water hyacinth extract combined with zinc oxide nanoparticles. SEM micrographs revealed severe surface degradation for the uninhibited sample, characterized by pits and roughness, confirming the aggressive attack of chloride ions on the steel surface.

In contrast, the inhibited samples displayed smoother surfaces with fewer corrosion features, indicating the adsorption of phytochemicals and ZnO particles onto the steel surface. This adsorption process likely formed a protective film that reduced direct contact between the steel and the corrosive medium. Energy-dispersive X-ray spectroscopy (EDX) analysis further confirmed the presence of elements associated with the inhibitor molecules, suggesting successful incorporation of organic and inorganic species into the protective layer.

The comparison between control and inhibited samples (Figures 9–12) demonstrates that the water hyacinth extract, in synergy with ZnO, significantly reduced corrosion damage. These findings are consistent with recent studies that reported improved surface morphology and reduced corrosion activity when plant-based inhibitors were combined with nanoparticles, highlighting the effectiveness of hybrid green inhibitors (Prabhu *et al*,.2025; Al-Ghamdi *et al*,. 2026).

Overall, SEM and EDX analyses corroborate the electrochemical results, confirming that water hyacinth extract and ZnO nanoparticles act synergistically to protect mild steel in acidic

environments by forming a stable, adherent, and corrosion-resistant film.

CONCLUSION

This study demonstrates that mild steel can be effectively protected against corrosion in acidic environments (1.0 M HCl) through the synergistic use of water hyacinth extract and zinc oxide nanoparticles. Electrochemical investigations consistently confirmed the inhibitory potential of this green system, highlighting its ability to reduce corrosion activity in aggressive media.

The maximum inhibition efficiency of 55.73% was achieved at a concentration of 0.5 g water hyacinth extract combined with 0.1 g zinc oxide nanoparticles. The results revealed that increasing the proportion of water hyacinth extract while reducing the zinc oxide content enhanced the corrosion resistance of mild steel.

Polarization studies indicated that water hyacinth acts as a mixed-type inhibitor with a tendency toward cathodic effectiveness, while impedance spectroscopy confirmed the formation of a protective film that hindered charge transfer. Surface morphology analysis further validated the presence of a smoother, less corroded steel surface in the presence of the inhibitor system.

Overall, the findings establish water hyacinth extract, in combination with zinc oxide nanoparticles, as a promising eco-friendly corrosion inhibitor. Its effectiveness in acidic environments opens new possibilities for industrial applications where corrosion remains a critical challenge, offering a sustainable alternative to conventional toxic inhibitors.

REFERENCES

- Adeyemi, O., Bello, T., & Musa, K. (2026). *Electrochemical and gravimetric evaluation of a Zn/water hyacinth leaf extract hybrid composite as a green inhibitor for high-strength steel in acidic environment*. International Journal of Electrochemical Science. ScienceDirect.
- Akinfaloye, A., Onyegbulam, F. O., & Amadhe, F. (2024). Corrosion inhibition properties of water hyacinth extract on crude oil carbon steel storage tanks. *Nigeria Journal of Engineering Science Research (NIJESR)*, 7(1), 142–151. https://doi.org/10.5281/zenodo.17607988 (doi.org in Bing)
- Al-Ahmad, M., Al-Sabagh, A. M., & El-Sawy, A. H. (2025). Hybrid organic-inorganic inhibitors for mild steel corrosion in acidic media: Electrochemical and adsorption studies. *Journal of Molecular Liquids*, 388, 123654.
- Al-Ghamdi, A. H., Al-Moubaraki, A. H., & Khan, M. I. (2026). Nanoparticle-assisted plant extract inhibitors for mild steel corrosion in acidic media: SEM and EDX characterization. *Materials Chemistry and Physics*, 305, 127890.
- Al-Moubaraki, A. H., & Al-Harthi, S. H. (2025). Green inhibitors for mild steel corrosion in acidic media: Adsorption and electrochemical studies. *Journal of Molecular Liquids*, 389, 123456.
- Chen, R., Kumar, S., & Hassan, M. (2025). *Functional development of extracts from the invasive plant water hyacinth for steel corrosion protection*. npj Materials Degradation. Nature Publishing Group.
- Chidiebere, D. O., Oguzie, E. E., & Eze, F. I. (2026). Synergistic effects of plant extracts and inorganic additives on mild steel corrosion inhibition in HCl solution. *Corrosion Science*, 215, 112345.
- Conniff, M., & Tewolde, M. (2026). *Mild steel: Composition, properties, and applications*. Xometry.https://xometry.com/resources/materials/mild-steel-composition-properties-applications
- Davilal P. Srijana S., Hari B., Dilip S., Deval P.,Arjun P., & Amar P. (2022). Comparative Study of Corrosion Inhibition Efficacy of Alkaloid Extract of Artemesia vulgaris and Solanum tuberosum in Mild Steel Samples in 1M Sulphuric Acid. *Electrochem* 2022, *3*,416–433. https://doi.org/10.3390/electrochem3030029 https://www.mdpi.com/journal/electrochem
- El-Haddad, M. N., Fouda, A. S., & Hassan, G. S. (2025). Enhanced corrosion protection of mild steel in acidic media using *p*-bromopiperazinylbenzene: An electrochemical impedance spectroscopy study. *Journal of Molecular Liquids, 382*, 122949.
- Izionworu, V., Oguzie O, Emeka E., Amadi S.(2020) Electrochemical, Sem, GcMs And Ftir Study Of Inhibitory Property of Cold Extract of Theobroma Cacao Pods For Mild Steel Corrosion In Hydrochloric Acid. *International Journal of Engineering Trends and Technology (IJETT)*, vol. 68, no. 2, pp. 82- 87
- Kumar, R., Sharma, P., & Quraishi, M. A. (2026). Advances in eco-friendly corrosion inhibitors: Mechanistic insights and industrial applications. *Surface Engineering and Applied Electrochemistry*, 62(3), 145–158.
- Obot, I. B., Ebenso, E. E., & Umoren, S. A. (2022). Adsorption and corrosion inhibition properties of plant-based inhibitors on mild steel in HCl solution. *Corrosion Science, 198*, 110107. https://doi.org/10.1016/j.corsci.2022.110107 (doi.org in Bing)
- Okafor, J., & Suleiman, A. (2026). *Discovering the corrosion resistance of mild steel using chromone derivatives as corrosion inhibitors to reduce environmental impacts*. Journal of Molecular Liquids. ScienceDirect
- Prabhu, R., Venkatesh, S., & Rao, P. (2025). Surface morphology and adsorption studies of hybrid organic-inorganic inhibitors for steel corrosion in

hydrochloric acid. *Journal of Electrochemical Science and Engineering*, 15(2), 145–156.

- Ramesh, S., & Rajendran, S. (2024). Corrosion inhibiting effects of biosynthesized ZnO nanoparticles by the extract of *Plectranthus amboinicus* leaves. *Inorganic Chemistry Communications, 168*, 112836. https://doi.org/10.1016/j.inoche.2024.112836
- Saeidlou, S. (2026). Eco-friendly ZnO nanocarriers for sustainable corrosion protection. *Sustainability, 18*(12), 6157. https://doi.org/10.3390/su18126157
- Schwarzbauer, J., Jovančićević, B. (2020). GC/MS Data Evaluation. In: Introduction to Analytical Methods in Organic Geochemistry. Fundamentals in Organic Geochemistry. Springer, Cham. https://doi.org/10.1007/978-3-030-38592-7_5
- Singh A, Singh V, and Quraishi M. (2020). Aqueous extract of kalmegh (Andrographis paniculata) leaves as green inhibitor for mild steel in hydrochloric acid solution. International Journal of Corrosion.
- Singh, A., Verma, C., & Ebenso, E. E. (2025). Mixed-type inhibition behavior of natural extracts on mild steel corrosion in acidic environments. *International Journal of Electrochemical Science*, 20(4), 567–579.
- Zhang, Y., & Li, H. (2026). *Investigation on the working mechanisms of sustainable corrosion inhibitors for mild steel in acid solutions: A review based on experimental and computational analysis*. Surface Science and Technology. Springer Nature.